IEEE Access
Multidisciplinary | Rapid Review | Open Access Journal

SPECIAL SECTION ON KEY ENABLING TECHNOLOGIES FOR PROSUMER ENERGY MANAGEMENT

Received July 5, 2020, accepted August 1, 2020, date of publication August 5, 2020, date of current version August 24, 2020.

Digital Object Identifier 10.1109/ACCESS.2020.3014341

An Integrated Transmission Expansion and Sectionalizing-Based Black Start Allocation of BESS Planning Strategy for Enhanced Power Grid Resilience

FANG YAO[1,2], (Member, IEEE), TAT KEI CHAU[2], (Member, IEEE), XINAN ZHANG[2], (Member, IEEE), HERBERT HO-CHING IU[2], (Senior Member, IEEE), AND TYRONE FERNANDO[2], (Senior Member, IEEE)

[1]School of Electric Power and Architecture, Shanxi University, Taiyuan 030013, China
[2]School of Electrical and Electronics and Computer Engineering, The University of Western Australia, Perth, WA 6009, Australia

Corresponding author: Fang Yao (y98122@hotmail.com)

ABSTRACT This paper proposes a new comprehensive integrated planning strategy for the resilience enhancement of power system, including determining the transmission expansion and sectionalizing-based optimal black start (BS) resources allocation of battery energy storage system (BESS) during extreme events. The planning model comprises of two stages, namely the normal stage and resilience stage. The first stage is to make the collaborative planning decisions, i.e., constructing transmission lines and installation of BESS as BS sources. The second stage minimizes the power system generation cost and load shedding cost under disaster conditions. The planning algorithm is developed to describe the uncertainty of transmission lines outage status, which can be affected by the normal stage expansion states. In algorithm ways, the model was solved with a duality-based column and constraint generation (D-CCG) method. Taking IEEE 30-bus and 39-bus system for examples and GUROBI/CPLEX was utilized to solve proposed model. Numerical cases show the effectiveness of the model and the superiority of the solution strategy.

INDEX TERMS Black start, battery energy storage system (BESS), load shedding, integrated planning, resilience enhancement, robust optimization.

NOMENCLATURE

Sets and Index

I	Index set of all buses.
G	Index set of generators.
T	Index set of time horizon.
L	Index set of transmission lines.
L^c	Index set of candidate lines.
M	Index set of BS candidate BESS.
N	Index set of NBS generators.
$\Omega()$	A damaged set defined by first stage plan of (u, g).
$F()$	A feasible region defined by first stage plan of (u, g) and the status of transmission network and candidates.
ptl	Index set of power transmission lines.

Constants and Parameters

Π_{L_C}	Maximum budget for transmission lines investment.
Π_{pd}	Maximum system load shedding.
B_{ptl}	Susceptance of transmission line ptl.
c_{ptl}	Investment cost for candidate line ptl.
c_n	Investment cost for BESS at candidate bus n.
c_{gi}^p	Unit generating cost of generator g at bus i.
c_i^d	Unit cost of load curtailment at bus i.
PD	Total system power load.
$p_{f1}^{\max}$	Maximal power flow of existing lines.
$p_{fl}^{\min}$	Minimal power flow of existing lines.
$p_{f2}^{\max}$	Maximal power flow of candidate lines.
$p_{f2}^{\min}$	Minimal power flow of candidate lines.
$p_{gi}^{\max}$	Maximum generation of generator g at bus i.
$p_{gi}^{\max}$	Minimum generation of generator g at bus i.
$pd_i^{\max}$	Maximum system load shedding at bus i.

The associate editor coordinating the review of this manuscript and approving it for publication was Junjie Hu.

$pd_i^{\min}$ Minimum system load shedding at bus i.
$\theta_{fptl}^{\max}$ Upper limits on phase angle at the sending end of line ptl.
$\theta_{fptl}^{\min}$ Lower limits on phase angle at the sending end of line ptl.
$\theta_{tptl}^{\max}$ Upper limits on phase angle at the receiving end of line ptl.
$\theta_{tptl}^{\min}$ Lower limits on phase angle at the receiving end of line ptl.
$SOC_i^{\max}$ Upper bound of state of charge of BESS at bus i.
$SOC_i^{\min}$ Lower bound of state of charge of BESS at bus i.
$r_{ch,i}^{\max}$ Maximal charge limits of BESS at bus i.
$r_{dch,i}^{\max}$ Maximal discharge limits of BESS at bus i.
η_{ch} BESS charging efficiency coefficient.
η_{dch} BESS discharging efficiency coefficient.
$\lambda_{ptl,i}$ Parameter presenting if the power flow on line ptl is from the sending end of the line ($\lambda_{ptl,i} = 1$) or not ($\lambda_{ptl,i} = -1$).

Decision Variables

u_{ptl} Binary variable (0/1) presenting if the candidate line ptl is chosen or not.
θ_{fptl}^t Phase angle at the initial end of line ptl in time t.
θ_{tptl}^t Phase angle at the terminal end of line ptl in time t.
p_{f1}^t Power flow of existing lines in time t.
p_{f1}^i Power flow of candidate lines in time t.
SOC_i^t State of charge of BESS at bus i in time t.
f_{ln} Integer variable indicates the number of flow units on transmission l flowing to island n.
a^l Binary variable presenting the outage status of existing lines.
a^{lc} Binary variable presenting the outage status of candidate lines.
q_n Binary variable presenting whether candidate BS of BESS n is chosen.
q_i Binary variable indicating whether bus i has candidate of BESS.
z_{mn} Binary variable indicating if node m is assigned to island n.
z_{in} Binary variable indicating whether bus i is assigned to island n.
y_{ln} Binary variable indicating whether a transmission line is assigned to island n.
u_{gi}^t Binary variable indicating whether generator gi is energized at time t.
s_{pl}^t Binary variable indicating whether transmission line pl is energized at time t.
pd_i^t Load shielding at bus i in period t.
p_{gi}^d Power output of generator gi at bus i in time t.
$r_{ch,i}^t$ The charge capacity of BESS at bus i in time t.
$r_{dch,i}^t$ The discharge capacity of BESS at bus i in time t.

Dual Variables:

u_1 Dual variable of power balance equation.
u_2 Dual variable of power flow on existing lines.
u_3 Dual variable of power flow on candidate lines.
u_4 Dual variable of minimal power flow on existing lines.
u_5 Dual variable of maximal power flow on existing lines.
u_6 Dual variable of minimal power flow on candidate lines.
u_7 Dual variable of maximal power flow on candidate lines.
u_8 Dual variable of minimal power flow on generator outputs.
u_9 Dual variable of maximal power flow on generator outputs.
u_{10} Dual variable of minimal load loss at all buses.
u_{11} Dual variable of maximal load loss at all buses.
u_{12} Dual variable of minimal limits of phase angles at initial ends of lines.
u_{13} Dual variable of maximal limits of phase angles at initial ends of lines.
u_{14} Dual variable of minimal limits of phase angles at terminal ends of lines.
u_{15} Dual variable of maximal limits of phase angles at terminal ends of lines.
u_{16} Dual variable of state of charge of BESS.
u_{17} Dual variable of minimal state of charge limits of BESS.
u_{18} Dual variable of maximal state of charge limits of BESS.
u_{19} Dual variable of maximal charging limits of BESS.
u_{20} Dual variable of maximal discharge limits of BESS.
u_{21} Dual variable of maximal system load loss.

I. INTRODUCTION

Since entering the 21st century, many countries speed up the pace of the development of power industry, cross-region and even cross-country power network, renewable energy development and grid interconnection, and the wide applications of electric vehicles, make the installed components, structures and coordinated control of power system more complex [1], [2]. Security, stability, economy and other issues of the system operation become more prominent. At the same time, extreme weather and natural disasters, as well as human and social instability, have further exacerbated the uncertainty in the development of the power system. As a result, power grid is still threatened by large-scale power outages. For example, in 2012 more than 1000,000 main electric wires and many substations were damaged by Hurricane Sandy in New York [3], [4]. In 2016, supercell thunderstorms and four tornadoes impacted the South Australian power network, which resulted in the loss of supply to 850,000 customers [5]. On 23 August 2017 a Category 3 hurricane, Typhoon Hato,

struck southern China, about 700,000 families suffered from power outage in Guangdong Province, China [6].

In this context, many electric power enterprises, companies, research institutions and universities have carried out a series of research and practice on the future development mode of electric power system, and put forward the concept of building resilient power system. The so-called resilient power system refers to the power system with adaptive flexible control and strong impact resistance [7], [8]. The system can ensure safe and stable operation no matter in the case of normal operation or short circuit fault. When the system encounters disturbance events, it has the ability to make corresponding preparation and prevention [9], [10]. The power system has the ability to fully resist, absorb, respond to and adapt to disturbance events. The power system has the ability to quickly return to a preset expected normal state after a disturbance event [11], [12].

Based on the resilience requirement of the power system, experts and scholars analyze the whole process of the power grid suffering from disturbance events, propose the response curve of the power grid during the disturbance, as shown in the figure 1, and point out that the research on the resilience enhancement of the power grid should consider three stages from the disturbance to the recovery of the power system: 1) Prevention Stage: corresponds to the period from 0 to t_1 illustrated in Figure 1; 2) Unfolding Stage: corresponds to the period from t_1 to t_3 illustrated in Figure 1; 3) Restoration stage: corresponds to the period from t_3 to t_4 illustrated in Figure 1.

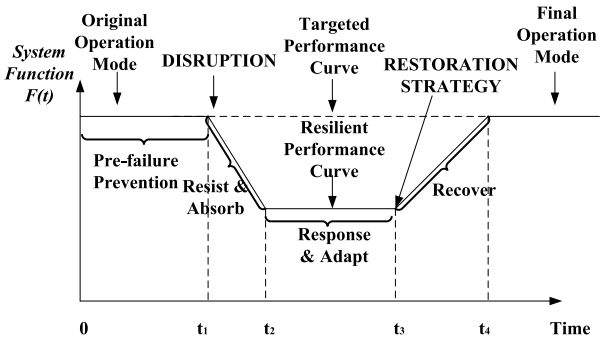

FIGURE 1. Response curve of resilient power grid after disturbance events.

The topic of how to improve the power system resilience is one that has existed for decades and has been dealt with in different ways. Nowadays, a large number of research achievements have been made on the three stages of resilience, which provide theoretical basis and reference methods for future researchers to study the resilience of power grid and enhance the resilience of power grid.

As for the prevention stage before failure, many studies tend to take effective preventive measures and control methods to reduce the probability of failure of power grid components and improve the power system resilience. Salman *et al.* [4] researched a targeted hardening framework to improve distribution support structures by evaluating power grid reliability. In [13], authors propose an optimal hardening strategy to improve the resilience of distribution system to protect against extreme weather events, which involves upgrading poles and vegetation management. A resilient distribution network planning problem (RDNP) to coordinate the hardening and distributed generation resource allocation with the objective of minimizing the system damage was proposed in [14]. Prior to the extreme weather events, smart grid technologies can enable the power system to fast locate power outages and restore loads more efficiently. Microgrids and distributed generator (DG) are able to maintain power supply to critical customers, or even support main grid splitting and recovery during a contingency [15]. Ehsan *et al.* [16] proposed a self-healing model to improve the overloading resilience of two islanded MGs. Farzin *et al.* [17] developed a hierarchical outage management strategy to improve the resilience of distribution system comprised of multiple MGs against disaster events.

The above researches mainly focus on the strategies prior to natural disasters. However, the strategies under a disruptive event were seldom developed in relatively existing research works. Huang *et al.* [18] proposed an integrated resilient model that integrates the preventive and emergency states for system resilience enhancement. In [19], the authors proposed a coordinated regional-district operation of integrated energy system (IES) for enhancing resilience in extreme conditions. A tri-level two-stage robust model was established to accommodate random outages caused by natural disasters in both natural gas and electricity generation and delivery systems. In [20], authors proposed a stochastic programming approach for increasing resiliency of a distribution system exposed to an approaching wildfire.

In terms of the restoration stage, it is necessary for the system decision maker to implement the recovery strategy to shorten the recovery time and improve the recovery efficiency. Conventional power system recovery can be generally divided into three stages, namely, the preparation stage, the system recovery stage and the fault recovery stage. A practical methodology for construction of system restoration strategies based on the concept of ''Generic Restoration Milestones (GRMs)'' was proposed in [21]. The decision support tool is expected to reduce the restoration time, thereby improving system reliability. A stochastic mixed integer linear program was researched to assess the impact of coordinating microgrids as a black start resource after a natural disaster [22]. Authors conclude that operable microgrids can provide sustainable benefits regardless of the natural disaster occurrence realized.

Even though the above research studies have focused on different technologies and strategies, few studies investigate sectionalizing-based black start (BS) resources allocation of BESS and generators start-up sequences, which are very effective strategies for resilience enhancement of power grid. Compared with conventional generators, BESS is able to supply electrical power for use during natural disasters. In addi-

tion, BESS can be used as distributed generators (DGs) which lead to a potential higher accessibility during the disturbance events. Capacity adequacy is another important key factor affecting the power system resilience during the disturbance events. A feasible generators start-up sequence will accelerate the power system black start process and further improve the system resilience by increasing the power grid capacity adequacy [23].

In this context, the proposed work presents a hierarchical integrated planning model to determine both transmission expansion and sectionalizing-based optimal BS allocation of BESS for power system resilience enhancement under extreme weather event. Moreover, the optimal non-black-start (NBS) generators restoration sequencing is also developed to provide a detailed power grid restoration process. The suggested integrated planning scheme extends the conventional optimal BS generators siting paradigm for power grid sectionalizing and accommodating BESS to further improve the power grid resilience in face of natural disasters.

The main contributions of this paper are as follows:

1) A robust model is developed for the coordinated planning of transmission lines and BS allocation considering the resilience constraints in which the BS allocation options depend on sectionalizing of the power grid.
2) A comprehensive restoration strategy is proposed for attaining a practical plan for power system resilience enhancement, including sectionalizing-based BS allocation of BESS, as well as determining the start-up sequences of NBS generators.
3) In the proposed robust integrated planning model, both the sectionalizing-based BS resources allocation of BESS and NBS generators restoration sequences are optimized simultaneously. Compared with existing relevant research works, the model must be modified by adding extra constraints. In addition, the n-k resilience criterion is included in the developed model.
4) The superiority of the proposed robust integrated planning over the sole transmission planning model is researched in this work.

The remainder of this paper is organized as follows. The resilience enhancement strategies during extreme whether events are introduced in Section II. The mathematical framework of the integrated planning strategy is provided in Section III. The corresponding algorithm is presented in Section IV. Two numerical results are presented in Section V. Section VI concludes the paper.

II. MODEL FORMULATION FOR RESILIENCE ENHANCEMENT

A. MULTISTAGE COLLABORATIVE PLANNING MODEL

Two-stage (i.e. normal, resilience) or tri-level (i.e. first, second, third) robust optimization models, also known as min-max-min sequential models, have been applied broadly in the power grid resilience enhancement problems [13], [18], [24]. In this paper, we develop a tri-level robust optimization model for resilient integrated planning as shown in Fig. 2. The power system operator decides the transmission expansion plan and the optimal BS resources allocation of BESS in the first level. In the second level, an extreme weather disaster, serving as the attacker, occurs and disrupts the power system. The damage of transmission network is maximized as the worst-case scenario. Finally, as the defender, the power system operator reacts to the worst-case scenario of an extreme event by adjusting the system load shedding and minimizing the system generation costs.

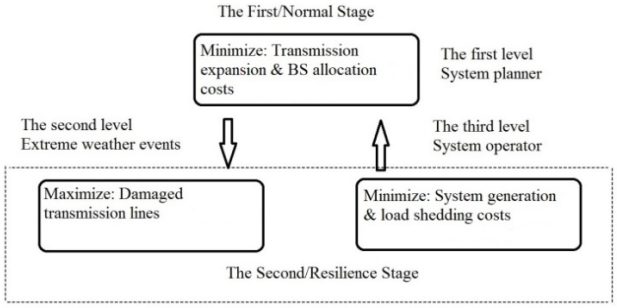

FIGURE 2. The developed multistage resilience model.

B. PRINCIPLES OF SECTIONALIZING-BASED BS RESOURCES ALLOCATION OF BESS

Black start is a necessary process that makes the power grid respond to power outages and restore power supply by self-starting BS resources. The four steps for black start are: preparation for black-start, restart all subareas and its controlled area, restoration of all subareas & interconnect them and full restoration of the whole system. Therefore, the power system operator should firstly divide the grid into several subareas by a Graph Sectionalizing model. Then a sectionalizing strategy will be defined that considers this new system status and satisfies all power system restoration constraints. According to the regional black-start scheme and the graph clustering techniques, we can acquire the partitioning islands by the following steps:

1) Graph representation of a power system in blackout:
   A bulk power system can be presented by an undirected graph with vertex set V and edge set E. The graph is an ordered pair G = (V, E) comprising a set V of vertices or nodes represents a bus together with a set E of edges or links represents a transmission lines between two buses, which are 2-element subsets of V.
2) Terminology and notation:
   The node subsets $N \subset I$ and $M \subset I$ are defined to represent the BS candidates of BESS and NBS generators, respectively. The graph sectionalizing is to choose a subset $N^* \subset N$ and partition the grid network into N^* subsections or islands consisted of one BS system. For convenience, the indices of BS units are reused as the indices of island, i.e. island n is the island having BS system n.

3) Generator start-up sequences:
Based on the optimal BS resources allocation of BESS and power grid sectionalizing strategy, we can determine the generators start-up sequences, in order to obtain the start time of each generator during the restoration period. As mentioned in lots of references, the piece-wise generation capacity curve is adopted in this work. A typical generator power output curve is given in Fig. 3.

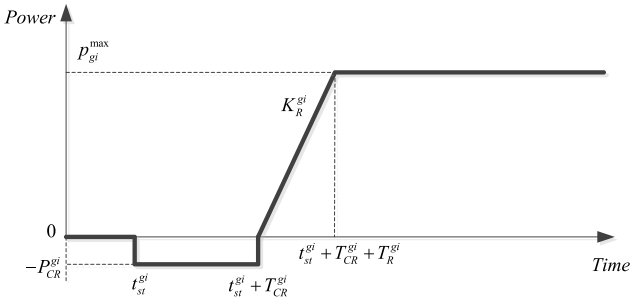

FIGURE 3. Typical generator power output curve.

In the above figure, $p_{gi}^{\max}$ (MW) is the maximal generator output power; p_{gi}^{CR} (MW) is the cranking power for NBS generator to absorb during the cranking period, therefore the cranking power can be considered as a negative generation; t_{st}^{gi} (min) is the start time for a generator to get energized; T_{CR}^{gi} (min) is the cranking time for NBS units; T_R^{gi} is the ramping time for both BS and NBS generators to reach its maximal power output. For BS generators, the cranking power consumption is zero and BS units can start immediately after the power outage, i.e. $t_{si}^{gi}=0$; K_R^{gi} is the ramping capacity.

4) Objective and constraints:
The objective of the sectionalizing strategy is to minimize the total BESS investment costs, whilst satisfying all the critical constraints.

$$Min: \sum_{n\in N} c_n q_n \tag{1}$$

$$\sum_{l\in\delta(m)} f_{\ln} = z_{mn},\ \forall m\in M,\ \forall n\in N \tag{2}$$

$$\sum_{l\in\delta(i)} f_{\ln} = 0,\ \forall i\in I\backslash(M\cup N), \forall n\in N \tag{3}$$

$$\sum_{l\in\delta(n)} f_{\ln} = \sum_{m\in M} z_{mn},\ \forall n\in N \tag{4}$$

$$\sum_{l\in\delta(i)} f_{\ln} = 0,\ \forall i\in N,\ \forall n\in N\backslash i \tag{5}$$

$$\sum_{n\in N} z_{mn} = 1,\ \forall m\in M \tag{6}$$

$$\sum_{n\in N} z_{in} \le 1,\ \forall i\in I\backslash M \tag{7}$$

$$-y_{\ln}|M| \le f_{\ln} \le y_{\ln}|M|, \forall l\in L\backslash\delta(n'), \quad n'\in N\backslash n, \forall n\in N \tag{8}$$

$$\sum_{l\in\delta(i)} y_{\ln} \le z_{in}|\delta(i)|, \forall n\in N, i\in I \tag{9}$$

$$z_{in} \le q_n,\ \forall i\in I, \forall n\in N \tag{10}$$

$$y_{\ln} \le q_n,\ \forall l\in L, \forall n\in N \tag{11}$$

$$y_{\ln} = 1-q_i,\ \forall i\in N, l\in\delta(i), n\in N\backslash i \tag{12}$$

$$\sum_{gi\in G}(p_{gi}^t + P_{CR}^{gi}(u_{BSgi}-u_{gi}^t)) - \sum_{pl\in L}\sum_{i\in I}\lambda_{pl,i}p_{f1}^t = d_i^t + r_{ch,i}^t/\eta_{ch} - r_{dch,i}^t\eta_{dch} + pd_i^t,\ \forall i\in I, \quad \forall gi\in G,\ \forall t\in T \tag{13}$$

$$0\le p_{gi}^{\tau} \le p_{gi}^{\max}u_{gi}^t,\ \forall gi\in G, \quad \forall\tau\in\left\{t,t+1,\ldots,t+T_{CR}^{gi}+1\right\} \quad \forall t\in T\cup\{0\} \tag{14}$$

$$p_{gi}^t - p_{gi}^{t-1} \le K_R^{gi},\ \forall gi\in G,\ \forall t\in T \tag{15}$$

$$p_{f1}^t = B_{pl}(\theta_{fpl}^t - \theta_{tpl}^t)s_{pl}^t,\ \forall pl\in L,\ \forall t\in T \tag{16}$$

$$\theta_{fpl}^{\min} \le \theta_{fpl}^t \le \theta_{fpl}^{\max},\ \forall pl\in L,\ \forall t\in T \tag{17}$$

$$\theta_{tpl}^{\min} \le \theta_{tpl}^t \le \theta_{tpl}^{\max},\ \forall pl\in L,\ \forall t\in T \tag{18}$$

$$SOC_i^t = SOC_i^{t-1} + r_{ch,i}^t - r_{dch,i}^t,\ \forall i\in I, \quad \forall t\in T \tag{19}$$

$$SOC_i^{\min} \le SOC_i^t \le SOC_i^{\max},\ \forall i\in I, \quad \forall t\in T \tag{20}$$

$$r_{ch,i}^t \le r_{ch,i}^{\max},\ \forall i\in I,\ \forall t\in T \tag{21}$$

$$r_{dch,i}^t \le r_{dch,i}^{\max},\ \forall i\in I,\ \forall t\in T \tag{22}$$

$$\sum_{i\in I} pd_i^t \le \prod_{pd},\ \forall i\in I,\ \forall t\in T \tag{23}$$

Eqn. (1) is the objective function for minimizing the BS units of BESS procurement costs. In (1), $q\in\{0,1\}$ is the decision variable presenting whether candidate BS unit n is chosen. Eqns. (2)-(4) are the transmission path balance constraints for nodes with an NBS generators, without any generators, and with a BS generator, respectively. $f_{\ln}$ is a integer variable indicates the number of unit flows on transmission l flowing to island n. These constraints ensure that there are no isolated buses, i.e. the buses in subsections are connected. In (2), $z_{mn}\in\{0,1\}$ is a binary variable presenting if node i unit is assigned to island n, then one unit flow is injected at NBS bus i and is subtracted at BS bus n. In (4), $\sum_{m\in M} z_{mn}$ represents the total number of NBS generators assigned to BS generator n. Eqn. (5) ensures that bus n can be used as an intermediate bus if the BS unit candidate n is not selected. Eqns. (6)-(7) require that each bus not be assigned to multiple subsections. Eqns. (8)-(12) require that the subsections are both pairwise node-disjoint and pairwise edge-disjoint. Eqn. (13) is the bus power balance constraint, $u_{gi}^t\in\{0,1\}$ is the decision variable presenting whether generator gi is energized at time t. Eqn. (14) ensures that the generators power output cannot be positive for at least T_{CR}^{gi} units of time

after the generator is energized. The generator ramping rate capacity is expressed by constraint (15). Eqn. (16) represents power flow on existing transmission lines, $s_{pl}^t \in \{0, 1\}$ is the decision variable presenting whether line pl is energized at time t. Eqns. (17) and (18) represent the phase angles limit at the initial ends and terminal ends of the transmission lines, respectively. Eqn. (19) describes the charging and discharging process of the BESS. Eqn. (20) restricts the capacity for the State-of-Charge (SOC) of BESS. Eqns. (21) and (22) introduces the charging and discharging rate limitations of BESS. Eqn. (23) gives the required load loss budget.

III. FORMULATION OF THE RESILIENCE-CONSTRAINTED MODEL

The proposed multistage collaborative planning model of transmission expansion and optimal BS allocation discussed in Section-2 is mathematically formulated in this section. The first stage of the strategy takes the minimum transmission construction and BS allocation costs as the optimization objective; the second stage minimizes power system operation and load loss costs under the extreme outage condition:

$$\min\Big(\sum_{ptl\in L^C} c_{ptl}u_{ptl} + \sum_{n\in N} c_n q_n \quad \max_{\Omega(u,q)}\min_{F(u,q,a^l,a^{lc})}\Big(\sum_{gi\in G} c_{gi}^p p_{gi}^t + \sum_{i\in I} c_i^d pd_i^t\Big)\Big) \tag{24}$$

$$Subject\ to: \sum_{ptl\in L^C} c_{ptl}u_{ptl} \le \prod_{L^C} \tag{25}$$

Eqn. (2)-(23)

$$\left(u_{ptl}, q_n\right) \in \{0, 1\} \tag{26}$$

Where :

$$\Omega(x) = \left\{ \sum_{j=1}^{n_L} a_j^l + \sum_{j=1}^{n_{LC}} a_j^{lc} \ge n_L + n_{LC} - k \right. \tag{27}$$

$$u_{ptl}{}_{ptl\in L^c} + a^{lc} \ge 1 \tag{28}$$

$$\left.\left(a^l, a^{lc}\right) \in \{0, 1\}\right\} \tag{29}$$

$$F(u, q, a^l, a^{lc}) = \begin{cases} \sum_{gi\in G} p_{gi}^t - \sum_{ptl\in L}\sum_{i\in I} \lambda_{ptl,i} p_{f1}^t \\ -\sum_{ptl\in L^c}\sum_{i\in I} \lambda_{ptl,i} p_{f2}^t \end{cases}$$
$$= d_i^t + r_{ch,i}^t/\eta_{ch} - r_{dch,i}^t\eta_{dch} + pd_i^t,$$
$$\forall i \in I, \forall gi \in G, \forall t \in T \tag{30}$$

$$p_{f1}^t = \left[a^l\right] B_{ptl}(\theta_{fptl}^t - \theta_{tptl}^t), \forall ptl \in L, \forall t \in T \tag{31}$$

$$p_{f2}^t = \left[u_{ptl}\right]\left[a^{lc}\right] B_{ptl}(\theta_{fptl}^t - \theta_{tptl}^t),$$
$$\forall ptl \in L^c, \forall t \in T \tag{32}$$

$$p_{f1}^{\min} \le p_{f1}^t \le p_{f1}^{\max}, \forall ptl \in L, \forall t \in T \tag{33}$$

$$p_{f2}^{\min} \le p_{f2}^t \le p_{f2}^{\max}, \forall ptl \in L^c, \forall t \in T \tag{34}$$

$$p_{gi}^{\min} \le p_{gi}^t \le p_{gi}^{\max}, \forall gi \in G, \forall t \in T \tag{35}$$

$$pd_i^{\min} \le pd_i^t \le pd_i^{\max}, \forall i \in I, \forall t \in T \tag{36}$$

$$\theta_{fptl}^{\min} \le \theta_{fptl}^t \le \theta_{fptl}^{\max}, \forall ptl \in (L \cup L^c), \forall t \in T \tag{37}$$

$$\theta_{tptl}^{\min} \le \theta_{tptl}^t \le \theta_{tptl}^{\max}, \forall ptl \in (L \cup L^c), \forall t \in T \tag{38}$$

$$SOC_i^t = SOC_i^{t-1} + r_{ch,i}^t - r_{dch,i}^t, \forall i \in I, \forall t \in T \tag{39}$$

$$SOC_i^{\min} \le SOC_i^t \le SOC_i^{\max}, \forall i \in I, \forall t \in T \tag{40}$$

$$r_{ch,i}^t \le r_{ch,i}^{\max}, \forall i \in I, \forall t \in T \tag{41}$$

$$r_{dch,i}^t \le r_{dch,i}^{\max}, \forall i \in I, \forall t \in T \tag{42}$$

$$\left.\sum_{i\in I} pd_i^t \le \prod_{pd}, \forall i \in I, \forall t \in T\right\} \tag{43}$$

The objective (24) is to minimize the total investment and system operation costs under the worst damaged condition. Eqn. (25) restricts the transmission construction investment. Eqn. (26) $(u_{ptl}, q_n) \in \{0, 1\}$ are two decision varibles representing whether a construction decision is carried out or not, which will be used in the second stage. Eqns. (27)-(29) find the uncertainty set of damaged scenarios for the given construction decisions in the first stage. Eqn. (27) picks n_L and n_{LC} to indicate the numbers of existing power lines and candidate power lines, respectively; and k is the estimated maximal number of failed transmission lines. On the left-hand side of Eqn. (27), a_j^l and a_j^{lc} are presented to indicate the damaged status of existing lines, candidate lines under a extreme event, respectively. Eqn. (28) imposes the damage status of candidate transmission lines. If a line was not constructed ($u_{ptl} = 0$), it will not be failed ($a^{lc} = 1$). Eqns. (30)-(43) define the system operation set that minimizes the power generation and load loss costs due to the worst damaged case. In Eqns. (31) and (32), the variables in brackets represent binary varibles of these equations. Eqns. (31) and (32) reflect power flow on existing power lines and candidate power lines, respectively. Eqns. (33) and (34) limit power flow on existing and candidate lines, respectively. Eqn. (35) limits the power output of generators. Eqn. (36) imposes the lower bound and upper bound of load curtailment. Eqns. (37) and (38) enforce the phase angles limitations at the initial ends and terminal ends of transmission lines, respectively. Eqn. (39) expresses the charge and discharge process of the BESS. Constraint (40) imposes the limits for the State-of-Charge (SOC) of BESS. The charge and discharge rate limits of BESS are enforced in Eqns. (41) and (42). Eqn. (43) gives the total load curtailment budget.

IV. SOLUTION METHODOLOGY

The coordinated planning model considering the n-2 resilience criterion proposed in this paper is a highly complex two-stage and three-level robust optimization model. On the one hand, the model is a mathematical programming problem containing a large number of integer variables, which is quite difficult to solve. On the other hand, the min-max-min structure cannot be directly solved. Here we introduce a more advanced algorithm that is the duality-based column and constraint generation (D-CCG) algorithm upgrading the primality-based column and constraint generation (P-CCG) algorithm [25], [26]. The model will be decomposed into investment master-problem and operation

sub-problem by using the D-CCG. The essential difference between D-CCG and P-CCG is the way reformulating the middle and lower levels into a problem with a single level, which is the sub-problem of the original model. In order to achieve the sub-problem, the KKT conditions are used in P-CCG for the lower level problem, whereas the dualization is used in D-CCG for the lower level problem. Compared with P-CCG, D-CCG proposes a recursive process in which fewer constraints and variables are added by the dual problem. In terms of the sub-problem, it will be solved by primal cuts, which is more efficient than other techniques such as Benders decomposition based on dual cuts.

A. SUB-PROBLEM

Given an integrated construction plan described by $\overline{u_{pl}}$ and $\overline{q_n}$ representing the construction of transmission lines and BS resources allocation, respectively, the sub-problem determines the damaged uncertainty set and minimizes the power generation and load loss costs under the worst damaged scenario.

$$\max_{\Omega(u,q)} \min_{F(u,q,a^l,a^{lc})} \left(\sum_{gi\in G} c^p_{gi} p^t_{gi} + \sum_{i\in I} c^d_i pd^t_i\right) \tag{44}$$

$$F(u,q,a^l,a^{lc}) = \begin{cases} \sum_{gi\in G} p^t_{gi} - \sum_{ptl\in L}\sum_{i\in I} \lambda_{ptl,i} p^t_{f1} \\ -\sum_{ptl\in L^c}\sum_{i\in I} \lambda_{ptl,i} p^t_{f2} \end{cases}$$

$$= d^t_i + r^t_{ch,i}/\eta_{ch} - r^t_{dch,i}\eta_{dch} + pd^t_i, \forall i \in I,$$

$$\forall m,n \in G,\ \forall t \in T : u_1 \tag{45}$$

$$p^t_{f1} = \left[a^l\right] B_{ptl}(\theta^t_{fptl} - \theta^t_{tptl}),$$

$$\forall ptl \in L,\ \forall t \in T : u_2 \tag{46}$$

$$p^t_{f2} = \left[\overline{u_{ptl}}\right]\left[a^{lc}\right] B_{ptl}(\theta^t_{fptl} - \theta^t_{tptl}),$$

$$\forall ptl \in L^c,\ \forall t \in T : u_3 \tag{47}$$

$$p^{\min}_{f1} \le p^t_{f1} \le p^{\max}_{f2},\ \forall ptl \in L,\ \forall t \in T : u_4, u_5 \tag{48}$$

$$p^{\min}_{f2} \le p^t_{f2} \le p^{\max}_{f2},\ \forall ptl \in L^c,\ \forall t \in T : u_6, u_7 \tag{49}$$

$$p^{\min}_{gi} \le p^t_{gi} \le p^{\max}_{gi},\ \forall gi \in G,\ \forall t \in T \quad : u_8, u_9 \tag{50}$$

$$pd^{\min}_i \le pd^t_i \le pd^{\max}_i,\ \forall i \in I,\ \forall t \in T : u_{10}, u_{11} \tag{51}$$

$$\theta^{\min}_{fptl} \le \theta^t_{fptl} \le \theta^{\max}_{fptl},\ \forall ptl \in (L \cup L^c),\ \forall t \in T : u_{12}, u_{13} \tag{52}$$

$$\theta^{\min}_{tptl} \le \theta^t_{tptl} \le \theta^{\max}_{tptl},\ \forall ptl \in (L \cup L^c),\ \forall t \in T : u_{14}, u_{15} \tag{53}$$

$$SOC^t_i = SOC^{t-1}_i + r^t_{ch,i} - r^t_{dch,i},\ \forall i \in I,\ \forall t \in T : u_{16} \tag{54}$$

$$SOC^{\min}_i \le SOC^t_i \le SOC^{\max}_i,\ \forall i \in I,\ \forall t \in T : u_{17}, u_{18} \tag{55}$$

$$r^t_{ch,i} \le r^{\max}_{ch,i},\ \forall i \in I,\ \forall t \in T : u_{19} \tag{56}$$

$$r^t_{dch,i} \le r^{\max}_{dch,i},\ \forall i \in I,\ \forall t \in T \quad : u_{20} \tag{57}$$

$$\sum_{i\in I} pd^t_i \le \prod_{pd},\ \forall i \in I,\ \forall t \in T : u_{21} \tag{58}$$

Where :

$$\Omega(x) = \begin{cases} \sum_{sl=1}^{n_L} a^l + \sum_{slc=1}^{n_{LC}} a^{lc} \ge n_L + n_{LC} - k & (59) \\ u_{ptl\in L^c}^{pl} + a^{lc} \ge 1 & (60) \\ \left(a^l, a^{lc}\right) \in \{0,1\} \end{cases} \tag{61}$$

The dual problem of the lower level problem can be expressed as:

$$\begin{aligned} \max_{u1-u21} & \sum_{i\in I} d^t_i u_1 + \sum_{l\in L^c} p^{\min}_{f1} u_4 - \sum_{p^{\max}_{f1}} u_5 + \sum_{ptl\in L} p^{\min}_{f2} u_6 \\ & - \sum_{ptl\in L} p^{\max}_{f2} u_7 + \sum_{n\in G} p^{\min}_{gi} u_8 - \sum_{n\in G} p^{\max}_{gi} u_9 \\ & + \sum_{i\in I} pd^{\min}_i u_{10} - \sum_{i\in I} pd^{\max}_i u_{11} + \sum_{fptl\in L} \theta^{\min}_{fpl} u_{12} \\ & - \sum_{fptl\in L^c} \theta^{\max}_{fpl} u_{13} + \sum_{tptl\in L} \theta^{\min}_{tpl} u_{14} \\ & - \sum_{tptl\in L^c} \theta^{\max}_{tptl} u_{15} + \sum_{i\in I} SOC^{\min}_i u_{17} \\ & - \sum_{i\in I} SOC^{\max}_i u_{18} - \sum_{i\in I} r^{\max}_{ch,i} u_{19} \\ & - \sum_{i\in I} r^{\max}_{dch,i} u_{20} - \prod_{pd} u_{21} \end{aligned} \tag{62}$$

$$p^t_{gi} : u_1 - u_8 + u_9 \le \sum_{gi\in G} c^p_{gi} \tag{63}$$

$$pd^t_i : -u_1 - u_{10} + u_{11} + u_{16} \le \sum_{i\in I} c^d_i \tag{64}$$

$$p^t_{f1} : -\sum_{ptl\in L}\sum_{i\in I} \lambda_{ptl,i} u_1 + u_2 - u_4 + u_5 = 0 \tag{65}$$

$$p^t_{f2} : -\sum_{ptl\in L^c}\sum_{i\in I} \lambda_{ptl,i} u_1 + u_3 - u_6 + u_7 = 0 \tag{66}$$

$$\theta^t_{fptl} : -\left[a^l\right] B_{ptl} u_2 - \left[\overline{u_{ptl}}\right]\left[a^{lc}\right] B_{ptl} u_3 - u_{12} + u_{13} = 0 \tag{67}$$

$$\theta^t_{tptl} : \left[a^l\right] B_{ptl} u_2 + \left[\overline{u_{ptl}}\right]\left[a^{lc}\right] B_{ptl} u_3 - u_{14} + u_{15} = 0 \tag{68}$$

$$SOC^t_i : -u_{17} + u_{18} = 0 \tag{69}$$

$$r^t_{ch,i} : -u_1 + u_{19} = 0 \tag{70}$$

$$r^t_{dch,i} : u_1 + u_{20} = 0 \tag{71}$$

$$u_4 \sim u_{21} \ge 0 \tag{72}$$

Eqns. (67) and (68) contain bilinear terms which are $[a^l]u_2$ and $[a^{lc}]u_3$. Using standard approaches, the bilinear terms $a^l u_2$, $a^{lc} u_3$ can be replaced by β_2, β_3, respectively. Then the following linear constraints are introduced:

$$\beta_2 = u_2 - h_2 \tag{73}$$

$$-Ma^l \le \beta_2 \le Ma^l \tag{74}$$

$$-M(1-a^{l}) \le h_2 \le M(1-a^{l}) \tag{75}$$
$$\beta_3 = u_3 - h_3 \tag{76}$$
$$-Ma^{lc} \le \beta_3 \le Ma^{lc} \tag{77}$$
$$-M(1-a^{lc}) \le h_3 \le M(1-a^{lc}) \tag{78}$$

B. MASTER-PROBLEM

At the k^{th} iteration, for any $m < k$, variables $a^{l(m)}$, $a^{lc(m)}$ can be generated from the corresponding sub-problem, thus the master-problem can be presented in the following model:

$$\min_{u,q}\Big(\sum_{ptl\in L^C} c_{ptl}u_{ptl} + \sum_{n\in G} c_n q_n + \alpha\Big) \tag{79}$$
$$\sum_{ptl\in L^C} c_{ptl}u_{ptl} \le \prod_{L^C} \tag{80}$$
$$\sum_{l\in\delta(m)} f_{\ln} = z_{mn},\ \forall m \in M,\ \forall n \in N \tag{81}$$
$$\sum_{l\in\delta(i)} f_{\ln} = 0,\ \forall i \in I\backslash(M\cup N),\ \forall n \in N \tag{82}$$
$$\sum_{l\in\delta(n)} f_{\ln} = \sum_{m\in M} z_{mn},\ \forall n \in N \tag{83}$$
$$\sum_{l\in\delta(i)} f_{\ln} = 0,\ \forall i \in N,\ \forall n \in N\backslash i \tag{84}$$
$$\sum_{n\in N} z_{mn} = 1,\ \forall m \in M \tag{85}$$
$$\sum_{n\in N} z_{in} \le 1,\ \forall i \in I\backslash M \tag{86}$$
$$-\ y_{\ln}|M| \le f_{\ln} \le y_{\ln}|M|,\ \forall l \in L\backslash\delta(n'),\ n' \in N\backslash n,\ \forall n \in N \tag{87}$$
$$\sum_{l\in\delta(i)} y_{\ln} \le z_{in}|\delta(i)|,\ \forall n \in N, i \in I \tag{88}$$
$$z_{in} \le q_n,\ \forall i \in I,\ \forall n \in N \tag{89}$$
$$y_{\ln} \le q_n,\ \forall l \in L,\ \forall n \in N \tag{90}$$
$$y_{\ln} = 1 - q_i,\ \forall i \in N, l \in \delta(i), n \in N\backslash i \tag{91}$$
$$\sum_{gi\in G}(p^t_{gi} + P_{CR_{gi}}(u_{BSgi} - u^t_{gi})) - \sum_{ptl\in L}\sum_{i\in I}\lambda_{ptl,i}p^t_{f1} = d^t_i + r^t_{ch,i}/\eta_{ch} - r^t_{dch,i}\eta_{dch} + pd^t_i,\ \forall i \in I,\ \forall gi \in G,\ \forall t \in T \tag{92}$$
$$0 \le p^{\tau}_{gi} \le p^{\max}_{gi}u^t_{gi},\ \forall gi \in G,\ \forall \tau \in \{t, t+1, \ldots, t+T_{CR_g}+1\}\ \forall t \in T \tag{93}$$
$$p^t_{gi} - p^{t-1}_{gi} \le K_{R_g},\ \forall gi \in G,\ \forall t \in T \tag{94}$$
$$p^t_{f1} = B_{ptl}(\theta^t_{fptl} - \theta^t_{tptl})s^t_{ptl},\ \forall ptl \in L,\ \forall t \in T \tag{95}$$
$$\theta^{\min}_{fptl} \le \theta^t_{fptl} \le \theta^{\max}_{fptl},\ \forall ptl \in L,\ \forall t \in T \tag{96}$$
$$\theta^{\min}_{tptl} \le \theta^t_{tptl} \le \theta^{\max}_{tptl},\ \forall ptl \in L,\ \forall t \in T \tag{97}$$
$$SOC^t_i = SOC^{t-1}_i + r^t_{ch,i} - r^t_{dch,i},\ \forall i \in I,\ \forall t \in T \tag{98}$$
$$SOC^{\min}_i \le SOC^t_i \le SOC^{\max}_i,\ \forall i \in I,\ \forall t \in T \tag{99}$$
$$r^t_{ch,i} \le r^{\max}_{ch,i},\ \forall i \in I,\ \forall t \in T \tag{100}$$
$$r^t_{dch,i} \le r^{\max}_{dch,i},\ \forall i \in I,\ \forall t \in T \tag{101}$$
$$\sum_{i\in I} pd^t_i \le \prod_{pd},\ \forall i \in I,\ \forall t \in T \tag{102}$$
$$(u_{ptl}, q_n) \in \{0,1\} \tag{103}$$
$$\alpha \ge (\sum_{gi\in G} c^p_{gi}p^{t(m)}_{gi} + \sum_{i\in I} c^d_i pd^{t(m)}_i),\ m = 1, \ldots, k-1 \tag{104}$$
$$\begin{cases}\sum_{gi\in G} p^t_{gi} - \sum_{ptl\in L}\sum_{i\in I}\lambda_{ptl,i}p^{t(m)}_{f1} \\ -\sum_{ptl\in L^c}\sum_{i\in I}\lambda_{ptl,i}p^{t(m)}_{f2}\end{cases} = d^t_i + r^t_{ch,i}/\eta_{ch} - r^t_{dch,i}\eta_{dch} + pd^{t(m)}_i,\ m = 1, \ldots, k-1 \tag{105}$$
$$p^{t(m)}_{f1} = \left[\overline{a^{l}}^{(m)}\right]B_{ptl}(\theta^{t(m)}_{fptl} - \theta^{t(m)}_{tptl}),\ m = 1, \ldots, k-1 \tag{106}$$
$$p^{t(m)}_{f2} = [u_{ptl}]\left[\overline{a^{lc}}^{(m)}\right]B_{ptl}(\theta^{t(m)}_{fptl} - \theta^{t(m)}_{tptl}),\ m = 1, \ldots, k-1 \tag{107}$$
$$p^{\min}_{f1} \le p^{t(m)}_{f1} \le p^{\max}_{f2},\ m = 1, \ldots, k-1 \tag{108}$$
$$p^{\min}_{f2} \le p^{t(m)}_{f2} \le p^{\max}_{f2},\ m = 1, \ldots, k-1 \tag{109}$$
$$p^{\min}_{gi} \le p^{t(m)}_{gi} \le p^{\max}_{gi},\quad m = 1, \ldots, k-1 \tag{110}$$
$$pd^{\min}_i \le pd^{t(m)}_i \le pd^{\max}_i,\ m = 1, \ldots, k-1 \tag{111}$$
$$\theta^{\min}_{fptl} \le \theta^{t(m)}_{fptl} \le \theta^{\max}_{fptl},\ m = 1, \ldots, k-1 \tag{112}$$
$$\theta^{\min}_{tptl} \le \theta^{t(m)}_{tptl} \le \theta^{\max}_{tptl},\ m = 1, \ldots, k-1 \tag{113}$$
$$SOC^{t(m)}_i = SOC^{t-1(m)}_i + r^{t(m)}_{ch,i} - r^{t(m)}_{dch,i},\ m = 1, \ldots, k-1 \tag{114}$$
$$SOC^{\min}_i \le SOC^{t(m)}_i \le SOC^{\max}_i,\ m = 1, \ldots, k-1 \tag{115}$$
$$r^{t(m)}_{ch,i} \le r^{\max}_{ch,i},\ m = 1, \ldots, k-1 \tag{116}$$
$$r^{t(m)}_{dch,i} \le r^{\max}_{dch,i},\ m = 1, \ldots, k-1 \tag{117}$$
$$\sum_{i\in I} pd^{t(m)}_i \le \prod_{pd},\ m = 1, \ldots, k-1 \tag{118}$$

Eqns. (95) and (107) comprise the nonlinear parts which can be solved by applying the following big M constant:

$$\left|p^t_{f1} - B_{pl}(\theta^t_{fpl} - \theta^t_{tpl})\right| \le (1 - s^t_{pl})M,\quad m = 1, \ldots, k-1 \tag{119}$$
$$\left|p^{t(m)}_{f2} - \left[\overline{a^{lc}}^{(m)}\right]B_{pl}(\theta^{t(m)}_{fpl} - \theta^{t(m)}_{tpl})\right| \le (1 - u_{pl})M,\quad m = 1, \ldots, k-1 \tag{120}$$

C. SOLUTION ALGORITHM

By applying the D-CCG method, the two-level "max-min" sub-problem can be reformulated as a single level mixed-integer linear program (MILP). In terms of a given iteration, the master-problem can also be formulated as an MILP

problem by adding the corresponding additional variables and constraints. Both the sub-problem and master-problem can be solved by many solvers such as CPLEX and GUROBI. The detailed solution procedures is summarized in Fig. 4.

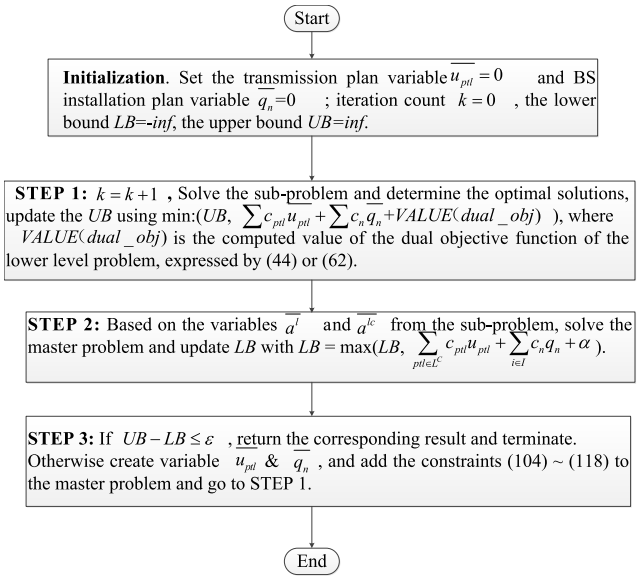

FIGURE 4. Solution process of the developed algorithm.

V. CASE STUDIES

The developed framework of is verified by IEEE 30-bus system [27] and IEEE 39-bus system [28]. The detailed transmission investment data can be found in reference [29]. The power generations coefficients, the load shedding coefficients, investments limits, and the characteristics of BESS are summarized in Table 1.

TABLE 1. Settings of parameters.

Quantity	Value	Unit
C_{gi}^{p}	30	M$/MWh
C_{i}^{d}	65	M$/MWh
$\prod_{L^C}$	41(IEEE-30) 187(IEEE-39)	M$
$\prod_{pd}$	[0%, 5%] of PD	MW
$SOC_i^{\min}$	20%	NA
$SOC_i^{\max}$	100%	NA
$r_{ch,i}^{\max}$	25%	NA
$r_{dch,i}^{\max}$	25%	NA

The following case studies were solved by the developed resilience enhancement model eqn. (24)-(43) including the proposed BS resources allocation eqn. (1)-(23), and by the proposed D-CCG algorithm. We only conduct the N-1 and N-2 resilience analysis as a result of the maximum computation time limitation which is specified to be 1 hour. By changing the estimated number of maximum failed components from 1 to 2, the two-stage resilient program was simulated for tests. For these two cases, two different, maximum system load shielding coefficients values of 0%, 5% of the total systems loads are assigned [18], respectively. However, the developed methodology can accommodate any values for the estimated number of maximum damaged component and the percentage of load shedding.

The proposed solution algorithm is implemented in MATLAB with GUROBI on a laptop with an Intel Core (TM) i7 2.60 GHz CPU and 8GB of memory.

A. IEEE 30-BUS SYSTEM

A small test system including 6 generators, 41 transmission lines, 21 system loads and a set of 41 candidate lines is illustrated for the joint planning programming model. This case study summarizes the sectionalizing-based BS resources allocation considering restoration sequence, transmission construction expansion planning, the load shielding, and total power grid operation costs of the two frameworks including 1) the optimal BS resources allocation 2) the robust sole transmission planning and 3) the robust coordinated planning.

1) OPTIMAL BS RESOURCES ALLOCATION AND NBS UNITS START UP SEQUENCING

The 4 candidate locations for BS units of BESS are bus1, bus2, bus13 and bus24 with the investment costs calculated from reference [30]. The optimal simulated installation plan is to set the BS resources of BESS at buses 1 and 2, while all the generators are regarded as NBS units. The statistics of the NBS units are taken from reference [31].

Fig. 5 shows the grid sectionalizing of the system. It is clear that the benchmark network is sectionalized into two subsections, each of which consists of a BS facility. The subsections included buses 1 and 2 are named as island I and island II, respectively.

The simulated optimal start-up sequences and restoration paths of NBS units within each subsection are shown in table 2.

TABLE 2. Restoration process of NBS generators of IEEE 30-bus system.

	Restoration sequences	Restoration paths
Island I	1--13--22--23	1--3--4--12--13
		4--12--16--17--10--22
		4--12--14--15--23
Island II	2--27	2--5--7--6--8--28--27

2) THE ROBUST SOLE TRANSMISSION PLANNING

Table 3 shows the transmission construction planning and total load shielding of the system together with system

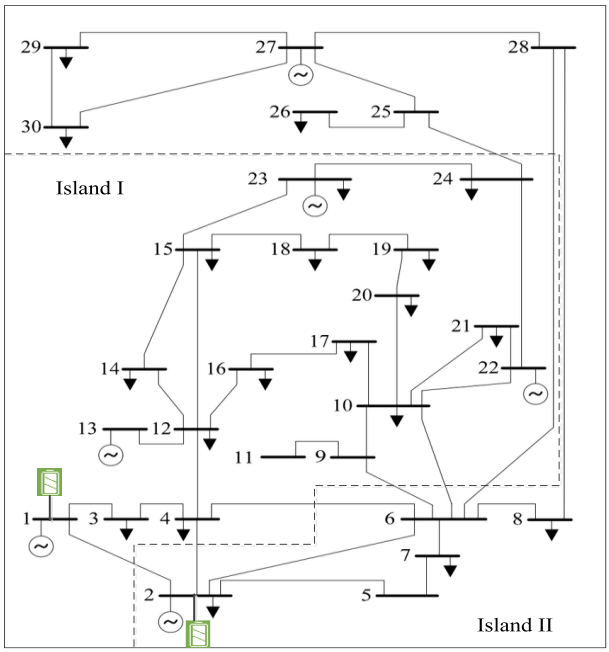

FIGURE 5. Sectionalizing of IEEE 30-bus system with two installed BESS.

operating costs considering the estimated k values ranging from 1 to 2. Different contingency coefficients k will result in different construction plans, which can future affect the system operation strategies. From the table, we easily notice that 1 candidate line was chosen to construct when k=1. The upward trend of constructed number of lines was obviously showed, and 6 new lines were built under the n-2 security criterion. It is observed that a higher k value causes a larger number of expansion lines. It is worth pointing out that n-1 security criterion requires no load shielding in power system. We can also find that the power system operation cost rises from $247.66 million to $328.32 million as the value of k goes up from 1 to 2, due to the increased load loss.

TABLE 3. IEEE 30-Bus Power System: Robust Sole Transmission Planning.

k	Transmission Expansion Plan (Lines No.)	Load Shedding (MW)	System Operation Cost (M$)
1	34	0	247.66
2	9,10,22,23,29,39	0.1075	328.32

3) THE ROBUST COORDINATED PLANNING

From Table 4, we can see that: 1) installation of BS resources of BESS leads to reducing the system load shielding and operating costs; and 2) compare with the robust sole transmission planning, the size of transmission expansion decreases of the coordinated model. The experimental results show that joint planning has its significant advantages that not only can enhance the system resilience but also provide cost savings for the system operator.

TABLE 4. IEEE 30-Bus power system: robust coordinated planning.

k	Transmission Expansion Plan (Lines No.)	BESS Plan (Bus No.)	Load Shedding (MW)	System Operation Cost ($10^6)
1	N/A	1，2	0	235.47
2	10,22,23,29,39	1，2	0.1038	322.54

B. IEEE 39-BUS SYSTEM

The applicability of the developed framework is indicated with a numerical experiment based on IEEE 39-bus system that comprises 10 thermal generators, 46 transmission lines and 46 candidate transmission circuits. The data of cranking powers, ramping rates and cranking times are taken from [28].

1) OPTIMAL BS RESOURCES ALLOCATION AND NBS UNITS START UP SEQUENCING

The 6 candidate locations for BS units of BESS are bus 2, bus 11, bus 29, bus 30, bus 31 and bus 34 with the investment costs calculated from literature [30]. The optimal simulated installation plan is to set the BS resources of BESS at buses 30, 31 and 34, while all the generators are all regarded as NBS units. Given the location of the BS sources, and based on the proposed sectionalizing-based planning, only three islands can be created which are named as island I, island II and island III. Also, as previously mentioned, one BS unit is included in each island i.e. generators at bus 30, 31 and 34 for the island I, island II and island III, respectively. Fig. 6 shows the graph sectionalizing of the IEEE 39-bus system.

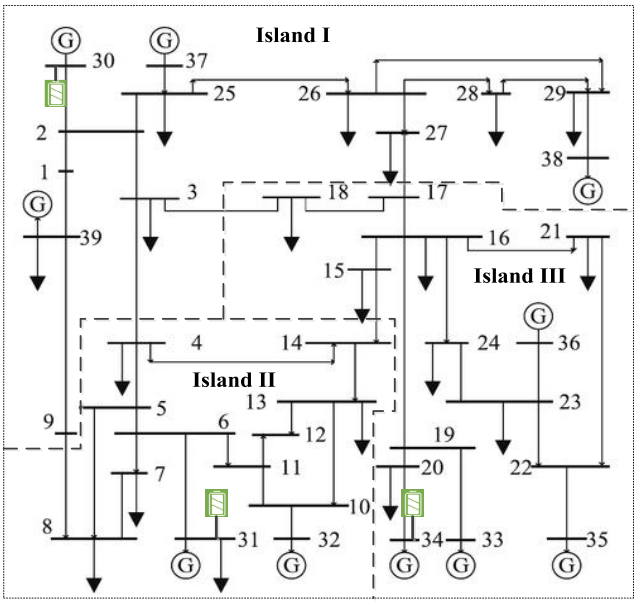

FIGURE 6. Sectionalizing of IEEE 39-bus system with three installed BESS.

The simulated optimal start-up sequences and restoration paths of NBS generator buses within every subsection are shown in table 5.

TABLE 5. Restoration process of NBS generators of IEEE 39-bus system.

	Restoration sequences	Restoration paths
Island I	30--37--39--38	30--2--25--37
		2--1--39
		25--26--29--38
Island II	31--32	31--6--11--10--32
		33--19--20--34
Island III	33--34--36--35	19--16--24--23--36
		23--22--35

2) THE ROBUST SOLE TRANSMISSION PLANNING

Table 6 gives an overview of the robust sole transmission lines planning model of both k values. Starting from k=1, the size of the construction plans is 2 lines. Then it increases gradually by the k values. When k=2, the size rises to 10 lines. Similar to the numerical experiment of IEEE 30-bus system, there is a rise in system load shielding to deal with the more transmission line failures. Because of the increased load loss, n-2 criterion incurs higher total operating costs.

TABLE 6. IEEE 39-Bus Power System: Robust sole transmission planning.

k	Transmission Lines Built (Line No.)	Load Shedding (MW)	System Operation Cost (M$)
1	14,16	0	262.29
2	6,21,23,27,29,31,33,37,38,42	0.2884	281.04

3) THE ROBUST COORDINATED PLANNING

The results of the robust collaborated planning are shown in Table 7. It is clear that if the BS resources allocations are considered in the proposed resilience constrained model, the system load shielding and the system operating costs will be affected. The results prove the advantage of the robust collaborative strategy from an economic perspective.

TABLE 7. IEEE 39-bus power system: Robust coordinated transmission planning.

k	Transmission Lines Built (Lines No.)	BESS Built (Bus No.)	Load Shedding (MW)	System Operation Cost (M$)
1	14	30,31,34	0	255.64
2	6,21,27,29,31,33 ,37	30,31,34	0.2871	277.35

VI. CONCLUSION

This paper models hierarchal interaction between integrated planning and resilience enhancement using tri-level robust optimization model to transmission expansion plan and decisions on BS facilities procurement, subject to resilience criterion. Integrated planning objective of cost minimization is employed at upper level, whereas the objective of optimizing system operation cost by altering its power flow and load shedding in the mid-lower level. The proposed collaborative planning model is tested on 30-bus and 39-bus system. Numerical experimental results demonstrate that the developed planning strategy can help the system operator to make the optimal construction plans to alleviate the impact of the natural disaster events. As can be seen from the case studies, when BS resources allocations of BESS are considered in the integrated planning model, the number of built transmission lines and system operation costs are reduced. Although building BESS infrastructure requires high investment costs and the payback period is long, it will lead to low load loss and operating costs. As a result, installation of BS resources of BESS is useful for enhancing power system resilience.

This work is formulated for the extreme weather events, and the proposed model could be potentially extended by incorporating cyber-physical attack.

REFERENCES

[1] J. Hu, G. Yang, C. Ziras, and K. Kok, "Aggregator operation in the balancing market through network-constrained transactive energy," *IEEE Trans. Power Syst.*, vol. 34, no. 5, pp. 4071–4080, Sep. 2019.
[2] J. Wu, J. Hu, X. Ai, Z. Zhang, and H. Hu, "Multi-time scale energy management of electric vehicle model-based prosumers by using virtual battery model," *Appl. Energy*, vol. 251, Oct. 2019, Art. no. 113312.
[3] Z. Bie, Y. Lin, G. Li, and F. Li, "Battling the extreme: A study on the power system resilience," *Proc. IEEE*, vol. 105, no. 7, pp. 1253–1266, Jul. 2017.
[4] A. M. Salman, Y. Li, and M. G. Stewart, "Evaluating system reliability and targeted hardening strategies of power distribution systems subjected to hurricanes," *Rel. Eng. Syst. Saf.*, vol. 144, pp. 319–333, Dec. 2015.
[5] *Extreme Weather and a Transforming Grid*. Accessed: Feb. 8, 2020. [Online]. Available: http://www.energynetworks.com.au/news/energy-insider/extreme-weather-and-transforming-grid
[6] L. Li, J. Yang, C.-Y. Lin, C. T. Chua, Y. Wang, K. Zhao, Y.-T. Wu, P. L.-F. Liu, A. D. Switzer, K. M. Mok, P. Wang, and D. Peng, "Field survey of typhoon hato (2017) and a comparison with storm surge modeling in macau," *Natural Hazards Earth Syst. Sci.*, vol. 18, no. 12, pp. 3167–3178, Nov. 2018.
[7] M. Chaudry, P. Ekins, and K. Ramachandran, "Building a resilient UK energy system," U.K. Res. Center, London, U.K., Res. Rep. REF UKERC/RR/HQ/2011/001, Apr. 2011.
[8] *Keeping the Country Running: Natural Hazards and Infrastructure*, Cabinet Office, London, U.K., 2011.
[9] *Arctic Resilience Report*, Stockholm Environ. Inst. Stockholm Resilience Centre, Arctic Council, Tromsø, Norway, 2016.
[10] T. Stoerk, G. Wagner, and R. E. T. Ward, "Policy brief—Recommendations for improving the treatment of risk and uncertainty in economic estimates of climate impacts in the sixth intergovernmental panel on climate change assessment report," *Rev. Environ. Econ. Policy*, vol. 12, no. 2, pp. 371–376, Jun. 2018.
[11] C. Rogers, C. Bouch, and S. Williams, "Resistance and resilience Paradigms for critical local infrastructure," *Proc. Inst. Civil Eng.*, vol. 165, no. 2, pp. 73–83, Jun. 2012.
[12] U.S. President, "Presidential policy directive-Critical infrastructure security and resilience," Presidential Policy Directive (PPD), Washington, DC, USA, Tech. Rep. PPD-21, 2013.
[13] S. Ma, B. Chen, and Z. Wang, "Resilience enhancement strategy for distribution systems under extreme weather events," *IEEE Trans. Smart Grid*, vol. 9, no. 2, pp. 1442–1451, Mar. 2018.
[14] W. Yuan, J. Wang, F. Qiu, C. Chen, C. Kang, and B. Zeng, "Robust optimization-based resilient distribution network planning against natural disasters," *IEEE Trans. Power Syst.*, vol. 7, no. 6, pp. 2817–2826, Nov. 2016.

[15] IEC MSB (Market Strategy Board), "Microgrids for disaster preparedness and recovery with electricity continuity plans and systems," Int. Electrotech. Commission, Geneva, Switzerland, White Paper, 2014, pp. 1–84.
[16] E. Pashajavid, F. Shahnia, and A. Ghosh, "Development of a self-healing strategy to enhance the overloading resilience of islanded microgrids," *IEEE Trans. Smart Grid*, vol. 8, no. 2, pp. 868–880, Mar. 2017.
[17] H. Farzin, M. Fotuhi-Firuzabad, and M. Moeini-Aghtaie, "Enhancing power system resilience through hierarchical outage management in multi-microgrids," *IEEE Trans. Smart Grid*, vol. 7, no. 6, pp. 2869–2879, Nov. 2016.
[18] G. Huang, J. Wang, C. Chen, J. Qi, and C. Guo, "Integration of preventive and emergency responses for power grid resilience enhancement," *IEEE Trans. Power Syst.*, vol. 32, no. 6, pp. 4451–4463, Nov. 2017.
[19] M. Yan, Y. He, M. Shahidehpour, X. Ai, Z. Li, and J. Wen, "Coordinated regional-district operation of integrated energy systems for resilience enhancement in natural disasters," *IEEE Trans. Smart Grid*, vol. 10, no. 5, pp. 4881–4892, Sep. 2019.
[20] D. N. Trakas and N. D. Hatziargyriou, "Optimal distribution system operation for enhancing resilience against wildfires," *IEEE Trans. Power Syst.*, vol. 33, no. 2, pp. 2260–2271, Mar. 2018.
[21] Y. Hou, C.-C. Liu, K. Sun, P. Zhang, S. Liu, and D. Mizumura, "Computation of milestones for decision support during system restoration," *IEEE Trans. Power Syst.*, vol. 26, no. 3, pp. 1399–1409, Aug. 2011.
[22] A. Castillo, "Microgrid provision of blackstart in disaster recovery for power system restoration," in *Proc. IEEE Int. Conf. Smart Grid Commun.*, Oct. 2013, pp. 534–539.
[23] T. C. Ly, J. N. Moura, and G. Velummylum, "Assessing the bulk power System's resource resilience to future extreme winter weather events," in *Proc. IEEE Power Energy Soc. Gen. Meeting*, Denver, CO, USA, Jul. 2015, pp. 1–4.
[24] C. Shao, M. Shahidehpour, X. Wang, X. Wang, and B. Wang, "Integrated planning of electricity and natural gas transportation systems for enhancing the power grid resilience," *IEEE Trans. Power Syst.*, vol. 32, no. 6, pp. 4418–4429, Nov. 2017.
[25] B. Zeng and L. Zhao, "Solving two-stage robust optimization problems using a column-and-constraint generation method," *Oper. Res. Lett.*, vol. 41, no. 5, pp. 457–461, Sep. 2013.
[26] L. Zhao and B. Zeng. *An Extract Algorithm for Two-Stage Robust Optimization With Mixed Integer Recourse Problems*. Accessed: Mar. 15, 2020. [Online]. Available: http://www.optimizationonline.org/DB_FILE/2012/01/3310.pdf
[27] M. Pai, *Energy Function Analysis for Power System Stability*. Boston, MA, USA: Kluwer, 1989.
[28] D. Wang, X. Gu, and G. Zhou, "Decision-making optimization of power system extended black-start coordinating unit restoration with load restoration," *Int. Trans. Electric. Energy Syst.*, vol. 27, no. 9, pp. 312–320, May 2017.
[29] C. Unsihuay-Vila, J. W. Marangon-Lima, A. C. Z. de Souza, I. J. Perez-Arriaga, and P. P. Balestrassi, "A model to long-term, multiarea, multistage, and integrated expansion planning of electricity and natural gas systems," *IEEE Trans. Power Syst.*, vol. 25, no. 2, pp. 1154–1168, May 2010.
[30] L. Xu, X. Ruan, C. Mao, B. Zhang, and Y. Luo, "An improved optimal sizing method for Wind-Solar-Battery hybrid power system," *IEEE Trans. Sustain. Energy*, vol. 4, no. 3, pp. 774–785, Jul. 2013.
[31] Y. Jiang, S. Chen, C.-C. Liu, W. Sun, X. Luo, S. Liu, N. Bhatt, S. Uppalapati, and D. Forcum, "Blackstart capability planning for power system restoration," *Int. J. Electr. Power Energy Syst.*, vol. 86, pp. 127–137, Mar. 2017.

FANG YAO (Member, IEEE) received the Ph.D. degree in electrical engineering from The University of Western Australia, Crawley, WA, Australia, in 2012. He is currently with the School of Electric Power and Architecture, Shanxi University. He is also with the School of Electrical and Electronics and Computer Engineering, The University of Western Australia. His research interests include power system resilience enhancement, smart grid, and artificial intelligence.

TAT KEI CHAU (Member, IEEE) received the B.Eng. degree (Hons.) in electronic and communication engineering from the City University of Hong Kong, Hong Kong, in 2010, and the master's and Ph.D. degrees in electrical engineering from The University of Western Australia (UWA), Perth, WA, Australia, in 2014 and 2019, respectively. From 2014 to 2015, he was an Electronics Testing Engineer, Hong Kong. Since November 2019, he has been a Postdoctoral Researcher with UWA. His research interests include power electronics, power system analysis and control, microgrids, demand-side management, smart grids, and renewable energy integration and forecasting.

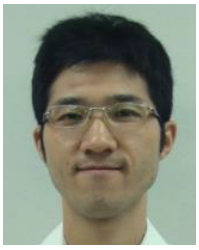

XINAN ZHANG (Member, IEEE) received the B.E. degree in electrical engineering and automation from Fudan University, China, in 2008, and the Ph.D. degree from Nanyang Technological University (NTU), Singapore, in 2014. He was a Postdoctoral Researcher with NTU and the University of New South Wales from 2014 to 2017. He was also a Lecturer with NTU from June 2017 to September 2019. Since September 2019, he has been with The University of Western Australia, as a Senior Lecturer. His research interests include electrical machine drives, control and modulation of power electronic converters, and management of hybrid energy storage systems.

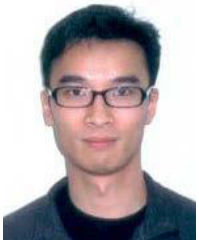

HERBERT HO-CHING IU (Senior Member, IEEE) received the B.Eng. degree (Hons.) in electrical and electronic engineering from The University of Hong Kong, Hong Kong, in 1997, and the Ph.D. degree from The Hong Kong Polytechnic University, Hong Kong, in 2000.

In 2002, he joined the School of Electrical, Electronic, and Computer Engineering, The University of Western Australia, Crawley, WA, Australia, as a Lecturer, where he is currently a Professor. He has authored over 100 articles. He is the coauthor of *Development of Memristor Based Circuits* (World Scientific, 2013). His research interests include power electronics, renewable energy, nonlinear dynamics, current sensing techniques, and memristive systems.

Dr. Iu serves as an Associate Editor for the IEEE TRANSACTIONS ON POWER ELECTRONICS, the IEEE TRANSACTIONS ON SMART GRID, the IEEE TRANSACTIONS ON NETWORK SCIENCE AND ENGINEERING, the IEEE TRANSACTIONS ON CIRCUITS AND SYSTEMS-II: EXPRESS BRIEFS, and IEEE ACCESS. He is the Co-Editor of *Control of Chaos in Nonlinear Circuits and Systems* (World Scientific, 2009). He also serves as the Deputy Editor-in-Chief for the IEEE JOURNAL ON EMERGING AND SELECTED TOPICS IN CIRCUITS AND SYSTEMS.

TYRONE FERNANDO (Senior Member, IEEE) received the Bachelor of Engineering (Hons.) and Ph.D. degrees in engineering from The University of Melbourne, in 1990 and 1996, respectively. In 1996, he joined the School of Electrical Electronic and Computer Engineering, The University of Western Australia, where he is currently a Professor. His research interests include power systems, renewable energy, state estimation, and biomedical engineering. He served as an Associate Editor for the IEEE TRANSACTIONS ON INFORMATION TECHNOLOGY IN BIOMEDICINE. He is currently an Associate Editor for the IEEE TRANSACTIONS ON CIRCUITS AND SYSTEMS-II: EXPRESS BRIEFS and IEEE ACCESS. He also served as a Guest Editor for *Optimal Control Applications and Methods* journal.